

1 **SUPPLEMENTARY INFORMATION**

2
3 **A resource-rational theory of set size effects in visual working memory**

4 Ronald van den Berg & Wei Ji Ma

5
6 **Contents**

7 Relation between Fisher information J and concentration parameter κ1

8 Theoretical proofs of some properties of the resource-rational model for local tasks.....1

9 Optimal decision rule for the change detection task8

10 Supplementary Tables8

11 Supplementary Figures.....9

12 Supplementary References11

13
14 **Relation between Fisher information J and concentration parameter κ**

15 Since we are only considering stimuli with circular domains, we assume that memory encoding
16 errors follow a Von Mises distribution with a concentration parameter κ ,

$$p(\varepsilon | \kappa) = \frac{1}{2\pi I_0(\kappa)} e^{\kappa \cos(\varepsilon)}, \tag{S.1}$$

17
18
19 where I_0 is the modified Bessel function of the first kind of order 0. We measure encoding precision
20 as Fisher information, J , which measures the performance of the best possible unbiased decoder.
21 Substituting Eq. (S.1) into the definition of Fisher information, we find that J and κ are one-to-one
22 related through

$$J = \kappa \frac{I_1(\kappa)}{I_0(\kappa)}. \tag{S.2}$$

23
24
25
26 Encoding precision J is a monotonically increasing function of κ and therefore invertible.
27 However, the inverse is not analytic, so we will use numerical inversion to compute the mapping
28 from J to κ when fitting models.

29 **Theoretical proofs of some properties of the resource-rational model for local tasks**

30 In this section, we prove three properties of the general model that we presented for “local” tasks,
31 i.e., tasks in which responses depend on a single item. This model is characterized by Eq. (11) in
32 the main text,

33
$$\bar{J}_{\text{optimal},i}(p_i; \lambda, \tau) = \underset{\bar{J}}{\operatorname{argmin}} \left(p_i \bar{c}_{\text{behavioral}}(\bar{J}; \tau) + \lambda \bar{J} \right), \quad (\text{S3})$$

34

35 where $\bar{J} \geq 0$, $p_i \in [0, 1]$, and $\lambda \geq 0$. We will also use the derivative of the expected total cost,

36
$$\bar{c}_{\text{total}}'(\bar{J}) = p_i \bar{c}_{\text{behavioral}}'(\bar{J}) + \lambda,$$

37

38 where $\bar{c}_{\text{behavioral}}'$ is the derivative of the expected behavioral cost.

39

40 We will now prove that the following three claims hold under very general assumptions about the
41 shape of the expected behavioral cost function in this model:

42 Claim 1. When neural coding is costly ($\lambda > 0$), it is optimal to encode items with a finite
43 amount of resource;

44 Claim 2. It is sometimes optimal to not encode a task-relevant item;

45 Claim 3. When each item is equally likely to be probed, $p_i = 1/N$, the optimal amount of
46 resource per item decreases with set size.

47

48 *Assumptions about the expected behavioral cost*

49 We construct our proofs under two intuitive and general assumptions about the expected
50 behavioral cost function $\bar{c}_{\text{behavioral}}(\bar{J})$:

51

52 Assumption 1. Expected behavioral cost is a monotonically decreasing function of
53 resource: whenever more resource is invested, the expected behavioral cost is lower. This
54 means that $\bar{c}_{\text{behavioral}}'(\bar{J}) \leq 0$ for all \bar{J} .

55

56 Assumption 2. A law of diminishing returns (Mankiw, 2004): when adding a bit of extra
57 resource, the resulting decrease in $\bar{c}_{\text{behavioral}}(\bar{J})$ is lower in magnitude when \bar{J} is higher.

58 This means that $\bar{c}_{\text{behavioral}}'(\bar{J})$ is monotonically increasing, i.e. $\bar{c}_{\text{behavioral}}''(\bar{J}) \geq 0$ for all \bar{J} .

59 As a consequence, $\bar{c}_{\text{behavioral}}'(\bar{J})$ takes its lowest value at $\bar{J} = 0$ and its largest as $\bar{J} \rightarrow \infty$.

60

61 Both assumptions are satisfied by the behavioral cost function that we used for fitting human data,
62 namely $c_{\text{behavioral}}(\varepsilon; \beta) = |\varepsilon|^\beta$. Examples of the expected behavioral cost function under this choice and
63 its first and second derivative are presented in Fig. S2.

64

65 *Three scenarios*

66 We now return to the problem of calculating \bar{J}_{optimal} , Eq. (S3). We are interested in the value

67 $\bar{J} \in [0, \infty)$ that minimizes the expected total cost, $\bar{c}_{\text{total}}(\bar{J})$. We separately consider the following

68 three scenarios: the minimum lies on the left boundary (0), on the right boundary (∞), or in
 69 between.

70

71 *Scenario 1: $\bar{c}_{\text{total}}(\bar{J})$ is monotonically decreasing across the domain of \bar{J} , so $\bar{J}_{\text{optimal}} \rightarrow \infty$.*

72 When does this happen? The monotonic decrease means that $\bar{c}_{\text{total}}'(\bar{J}) \leq 0$ for all \bar{J} , or

73 equivalently, $p_i \bar{c}_{\text{behavioral}}'(\bar{J}) \leq -\lambda$ for all \bar{J} . Since we assume $\bar{c}_{\text{behavioral}}'(\bar{J})$ to be monotonically

74 increasing (Assumption 2), its largest value is attained at $\bar{J} \rightarrow \infty$. Therefore, $p_i \bar{c}_{\text{behavioral}}'(\bar{J}) \leq -\lambda$

75 is equivalent to $p_i \bar{c}_{\text{behavioral}}'(\infty) \leq -\lambda$, or (using Assumption 1) $p_i |\bar{c}_{\text{behavioral}}'(\infty)| \geq \lambda$. This means that

76 it is optimal to invest infinite resource when p_i exceeds a critical value p_∞ :

77

$$\bar{J}_{\text{optimal}} = \infty \text{ when } p_i \geq p_\infty \equiv \frac{\lambda}{|\bar{c}_{\text{behavioral}}'(\infty)|}.$$

78

79 The condition $p_i \geq p_\infty$ is satisfied when $\lambda=0$. This makes sense: when neural cost plays no role,

80 there is no reason to not invest more. Other than that, the condition will rarely if ever be satisfied,

81 since every expected behavioral cost function that we can think of has the property

82 $|\bar{c}_{\text{behavioral}}'(\infty)| = 0$: as the amount of invested resource approaches infinity, there is no behavioral

83 benefit in investing more resource (note that p_∞ has a domain $[0, \infty)$, not $[0, 1]$). Therefore, unless

84 neural cost plays no role, we do not expect it to be optimal to invest an infinite amount of resource

85 in an item.

86 In tasks where p_i is one-to-one related to set size, the above result can be reformulated in

87 terms of set size. In particular, when probing probabilities are equal, $p_i = \frac{1}{N}$, the above result

88 implies that there exists a set size N_∞ (in general not an integer) below which it is optimal to invest

89 infinite resource in each item:

90

$$\bar{J}_{\text{optimal}} = \infty \text{ when } N \leq N_\infty \equiv \frac{1}{p_\infty} = \frac{|\bar{c}_{\text{behavioral}}'(\infty)|}{\lambda}.$$

91

92 *Scenario 2: $\bar{c}_{\text{total}}(\bar{J})$ is monotonically increasing across the domain of \bar{J} , so $\bar{J}_{\text{optimal}} = 0$.*

93 The monotonic increase means that $\bar{c}_{\text{total}}'(\bar{J}) \geq 0$ for all \bar{J} , or equivalently, $p_i \bar{c}_{\text{behavioral}}'(\bar{J}) \geq -\lambda$
 94 for all \bar{J} . Since we assume $\bar{c}_{\text{behavioral}}'(\bar{J})$ to be monotonically increasing (Assumption 2), its
 95 smallest value is attained at $\bar{J} \rightarrow \infty$. Therefore, $p_i \bar{c}_{\text{behavioral}}'(\bar{J}) \geq -\lambda$ is equivalent to
 96 $p_i \bar{c}_{\text{behavioral}}'(0) \geq -\lambda$, or (using Assumption 1) $p_i \left| \bar{c}_{\text{behavioral}}'(0) \right| \geq \lambda$. This means that it is optimal to
 97 invest no resource when p_i is smaller than or equal to a critical value p_0 :
 98

$$\bar{J}_{\text{optimal}} = 0 \text{ when } p_i \leq p_0 \equiv \frac{\lambda}{\left| \bar{c}_{\text{behavioral}}'(0) \right|}.$$

99
 100 A similar condition was derived in our earlier work (De Silva & Ma, 2018) for the case of a fixed
 101 total amount of resource (hard constraint).

102 The condition $p_i \leq p_0$ is satisfied when $p_i=0$. This makes sense: when an item never gets
 103 probed, one should not invest any resource. More generally, when probing probability is
 104 sufficiently low, the behavioral cost function is sufficiently shallow at 0, and neural cost is
 105 sufficiently important, it is not worth it to invest any resource on encoding. The expression for p_0
 106 also makes clear that the optimal amount of resource is never 0 when the slope of the behavioral
 107 cost function at 0 approaches $-\infty$.

108 In tasks where p_i is one-to-one related to set size, the above result can be reformulated in
 109 terms of set size. In particular, when probing probabilities are equal, $p_i = \frac{1}{N}$, the above result
 110 implies that there exists a set size N_0 (in general not an integer) beyond which it is optimal to not
 111 invest any resource in any item:
 112

$$\bar{J}_{\text{optimal}} = 0 \text{ when } N \geq N_0 \equiv \frac{1}{p_0} = \frac{\left| \bar{c}_{\text{behavioral}}'(0) \right|}{\lambda}.$$

113
 114 Intuitively, this means that when set size is too large, the chances of success are too low and one
 115 should not even try.
 116

117 *Scenario 3: $\bar{c}_{\text{total}}(\bar{J})$ has a stationary point, so \bar{J}_{optimal} is finite and nonzero.*

118 We will now consider the remaining scenario, which is the complement of Scenarios 1 and 2; in
 119 particular, we can take $\lambda > 0$ and $p_i > 0$. The stationary point of $\bar{c}_{\text{total}}(\bar{J})$ will always be a minimum,

120 since the second derivative $\bar{c}_{\text{total}}''(\bar{J})$ is equal to $\bar{c}_{\text{behavioral}}''(\bar{J})$, which is always positive
 121 (Assumption 2). At the minimum, we have $\bar{c}_{\text{total}}'(\bar{J}) = 0$, from which it follows that
 122 $\bar{c}_{\text{behavioral}}'(\bar{J}) = -\frac{\lambda}{p_i}$ at the minimum. Since the left-hand side is monotonically increasing as a
 123 function of \bar{J} (Assumption 2), the minimum is either a single point or a single interval, but there
 124 cannot be multiple disjoint minima. Graphically, this equation describes the intersection between
 125 $\bar{c}_{\text{behavioral}}'(\bar{J})$, which is a monotonically increasing function, and a flat line at a value $-\frac{\lambda}{p_i}$ (Fig.
 126 S3). The value of \bar{J} at which this intersection occurs necessarily increases with p_i .

127

128 *Three regimes for probing probability*

129 So far, we have assumed a given probing probability p_i . Now suppose that for a given $\bar{c}_{\text{behavioral}}(\bar{J})$
 130 and a given λ , we increase p_i from 0 to 1:

- 131 • The first regime is $p_i \leq p_0$. There, Scenario 2 applies and $\bar{J}_{\text{optimal}} = 0$: the item does not get
 132 encoded at all.
- 133 • The second regime is $p_0 < p_i < p_\infty$; there, Scenario 3 applies and \bar{J}_{optimal} monotonically
 134 increases with p_i .
- 135 • The third regime is $p_i \geq p_\infty$. There, Scenario 1 applies and $\bar{J}_{\text{optimal}} = \infty$: the item gets
 136 encoded with infinite resource.

137 Even though not each regime might exist, the model predicts across regimes that \bar{J}_{optimal} increases
 138 monotonically with p_i (Fig. 1F in main text).

139

140 *Three regimes for set size*

141 We can similarly examine the experimentally important special case of equal probing probabilities,

$$142 \quad p_i = \frac{1}{N}:$$

- 143 • The first regime is $N \leq N_\infty$. There, Scenario 1 applies and $\bar{J}_{\text{optimal}} = \infty$: all items are encoded
 144 with infinite resource.
- 145 • The second regime is $N_\infty < N < N_0$. There, Scenario 3 applies and \bar{J}_{optimal} monotonically
 146 decreases with N .
- 147 • The third regime is $N \geq N_0$. There, Scenario 2 applies and $\bar{J}_{\text{optimal}} = 0$: no items are encoded
 148 at all.

149 Even though not each regime might exist, the model predicts across regimes that \bar{J}_{optimal} decreases
 150 monotonically with N (Fig. 1G in main text).

151

152 *Conclusion*

153 In conclusion, given Eq. (S3) and two additional assumptions, we have proven the following:

- 154 • Investing infinite resource in an item is only optimal when $p_i |\bar{c}_{\text{behavioral}}'(\infty)| \geq \lambda$. In practice,
- 155 this might only happen when neural cost is unimportant ($\lambda=0$). This proves Claim 1.
- 156 • Investing no resource in an item is optimal when $p_i |\bar{c}_{\text{behavioral}}'(0)| \notin /$. This can happen even
- 157 when the probing probability p_i is nonzero. This proves Claim 2.
- 158 • \bar{J}_{optimal} is a monotonically increasing function of p_i . In particular, if $p_i = \frac{1}{N}$, then \bar{J}_{optimal} is a
- 159 monotonically decreasing function of N . This proves Claim 3.

160 All three results hold more generally than we have shown here: we can replace the neural cost
 161 term $/\bar{J}$ in Eq. (S3) by any function $c_{\text{neural}}(\bar{J})$ whose derivative is positive and monotonically
 162 increasing. The proofs proceed along the same lines.

163

164 *Special case: fixed-precision model*

165 For the fixed-precision model (variable-precision model with $\tau \downarrow 0$), Eqs. (9) and (10) in the
 166 main text combine to take the form

167

$$168 \quad \bar{c}_{\text{behavioral}}(J) = \int_{-\pi}^{\pi} c_{\text{behavioral}}(\varepsilon) \text{VM}(\varepsilon; J) d\varepsilon.$$

169

170 We wish to evaluate $p_0 \equiv \frac{\lambda}{|\bar{c}_{\text{behavioral}}'(0)|}$. First, we evaluate the derivative of $\bar{c}_{\text{behavioral}}(J)$ using the

171 chain rule:

172

$$173 \quad \frac{d\bar{c}_{\text{behavioral}}}{dJ} = \frac{d\bar{c}_{\text{behavioral}}}{dk} \frac{dk}{dJ}. \quad (\text{S4})$$

174

175 Using Eq. (S.1), the first factor is

176

$$\begin{aligned}
\frac{d\bar{c}_{\text{behavioral}}}{dk} &= \frac{d}{dk} \int_{-\rho}^{\rho} c_{\text{behavioral}}(e) \frac{1}{2\rho I_0(k)} e^{k \cos(e)} de \\
&= \frac{1}{2\rho} \int_{-\rho}^{\rho} c_{\text{behavioral}}(e) \frac{d}{dk} \left(\frac{1}{I_0(k)} e^{k \cos(e)} \right) de \\
&= \frac{1}{2\rho} \int_{-\rho}^{\rho} c_{\text{behavioral}}(e) \left(-\frac{I_0'(k)}{I_0(k)^2} e^{k \cos(e)} + \frac{\cos(e)}{I_0(k)} e^k \right) de \\
&= \frac{1}{2\rho} \int_{-\rho}^{\rho} c_{\text{behavioral}}(e) \left(-\frac{I_1(k)}{I_0(k)^2} e^{k \cos(e)} + \frac{\cos(e)}{I_0(k)} e^k \right) de.
\end{aligned} \tag{S5}$$

177

178

179 where in the last line we used $I_0'(k) = I_1(k)$ (see Eq. 9.6.27 in (Abramowitz & Stegun, 1972)).

180

We next evaluate the second factor in Eq. (S4) using Eq. (S.2):

181

$$\frac{dk}{dJ} = \left(\frac{dJ}{dk} \right)^{-1} = \left(\frac{d}{dk} \left(\frac{k I_1(k)}{I_0(k)} \right) \right)^{-1} = \left(\frac{k I_0(k)^2 - k I_1(k) I_0'(k)}{I_0(k)^2} \right)^{-1} = \left(k \left(1 - \frac{I_1(k)^2}{I_0(k)^2} \right) \right)^{-1}, \tag{S6}$$

182

183

184 where in the third equality, we used $\frac{d}{dk} (k I_1(k)) = k I_0(k)$ (see Eq. 9.6.28 in (Abramowitz &

185

186

187

188

Stegun, 1972)). We now combine Eqs. (S5) and (S6) into Eq. (S4), and the result in turn in the expression for p_0 . We also realize that the limit $J \downarrow 0$ is, using Eq. (S.2), equivalent to the limit $k \rightarrow 0$. Putting everything together, we find

189

$$p_0 = \lim_{k \downarrow 0} \left| \frac{k \left(1 - \frac{I_1(k)^2}{I_0(k)^2} \right)}{\frac{1}{2\rho} \int_{-\rho}^{\rho} c_{\text{behavioral}}(e) \left(-\frac{I_1(k)}{I_0(k)^2} e^{k \cos e} + \frac{\cos e}{I_0(k)} e^k \right) de} \right| = 0.$$

190

191

192

193

194

195

196

We conclude that in our theory for delayed estimation, assuming the expected behavioral cost function from the fixed-precision model, it is only optimal to invest no resource at all into an item when that item has zero probability of being probed.

197 **Optimal decision rule for the change detection task**

198 In our simulation of the change detection task, we assume that observers use a Bayesian decision
 199 rule. This rule is to report “change” whenever the posterior ratio of change presence over change
 200 absence exceeds 1,

$$201 \frac{p(\text{change present} | \mathbf{x}, \mathbf{y})}{p(\text{change absent} | \mathbf{x}, \mathbf{y})} > 1,$$

202
 203 where \mathbf{x} and \mathbf{y} denote the vectors of noisy measurements of the items in the first and second
 204 displays, respectively. Under the Von Mises noise assumption, and assuming a flat prior on change
 205 presence, this decision rule evaluates to (Keshvari, van den Berg, & Ma, 2013)

$$206 \frac{1}{N} \sum_{i=1}^N \frac{I_0(\kappa_{x,i}) I_0(\kappa_{y,i})}{I_0\left(\sqrt{\kappa_{x,i}^2 + \kappa_{y,i}^2 + 2\kappa_{x,i}\kappa_{y,i} \cos(y_i - x_i)}\right)} > 1,$$

208
 209 where $\kappa_{x,i}$ and $\kappa_{y,i}$ denote the concentration parameters of the Von Mises distributions associated
 210 with the observations of the items at the i^{th} location in the first and second displays, respectively.
 211 The predicted probability of a correct response for a given resource vector, $p(\text{error}|\bar{\mathbf{J}})$, is not
 212 analytic, but can easily be computed using Monte Carlo simulations.

213
 214

215 **Supplementary Tables**

216

217 *Table S1. Subject-averaged parameter estimates of the resource-rational model fitted to data*
 218 *from 11 previously published experiments. See Table 1 in main text for details about the*
 219 *experiments and references to the papers in which the experiments were originally published.*

Experiment	λ	τ	β
E1	$(4.48 \pm 0.66) \cdot 10^{-3}$	16.7±2.1	1.97±0.43
E2	$(2.66 \pm 0.28) \cdot 10^{-3}$	12.6±1.2	$(7.1 \pm 1.2) \cdot 10^{-2}$
E3	$(3.47 \pm 0.34) \cdot 10^{-3}$	17.9±2.1	0.228±0.040
E4	$(4.5 \pm 1.0) \cdot 10^{-3}$	7.3±1.7	0.176±0.064
E5	$(4.15 \pm 0.37) \cdot 10^{-3}$	18.5±3.0	0.426±0.089
E6	$(4.89 \pm 0.57) \cdot 10^{-3}$	7.6±1.4	0.66±0.14
E7	$(6.1 \pm 1.2) \cdot 10^{-3}$	5.7±1.6	1.64±0.90
E8	$(2.45 \pm 0.37) \cdot 10^{-3}$	28.8±7.0	1.53±0.67
E9	$(3.10 \pm 0.50) \cdot 10^{-3}$	23.8±2.4	1.52±0.63

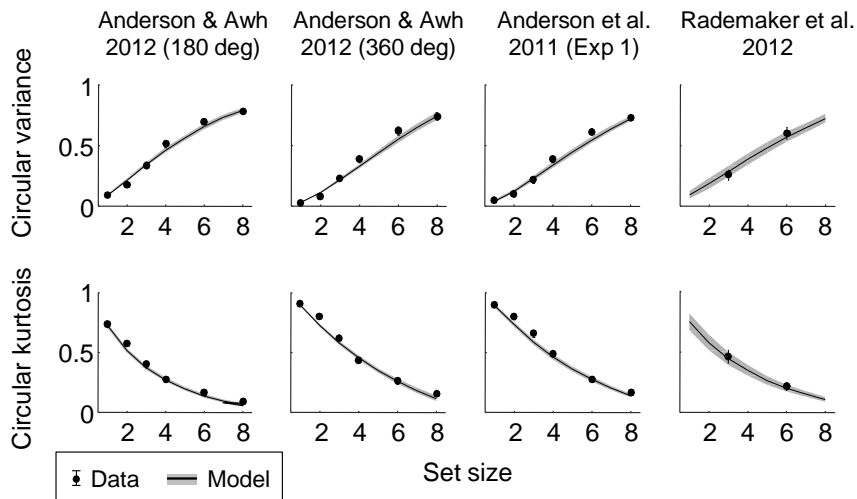
220
 221

222 *Table S2. Overview of AIC-based model comparison results reported in the main text, together*
 223 *with results from corresponding comparisons with five-fold cross validation (see Methods in main*
 224 *text). Each comparison is between the main version of the resource-rational model, Eq. (13), and*
 225 *the model listed in the first column of the table. Negative AIC differences and positive cross-*
 226 *validation log likelihood differences indicate an advantage of the resource-rational model over*
 227 *the alternative model. In all comparisons, these differences have opposite signs, which means that*
 228 *the AIC-based results are consistent with the cross-validation results.*

Model with which the main model is compared	AIC difference	Cross-validation log likelihood difference
Descriptive power-law model	-5.27 ± 0.70	2.59 ± 0.39
Descriptive fixed-resource model	-13.9 ± 1.4	8.4 ± 1.0
Descriptive unconstrained model	3.49 ± 0.93	-1.26 ± 0.49
Rational model variant: equal precision	-110 ± 10	56 ± 4.7
Rational model variant: $c_{\text{behavioral}} = \epsilon $	-14 ± 2.8	7.1 ± 1.4
Rational model variant: $c_{\text{behavioral}} = \epsilon^2$	-24.4 ± 4.1	12.2 ± 2.0
Rational model variant: $c_{\text{behavioral}} = -\cos(\epsilon)$	-19.5 ± 3.5	9.8 ± 1.8
Rational model variant: $c_{\text{behavioral}}$ as in Sims (2015)	-5.3 ± 1.8	4.7 ± 0.74

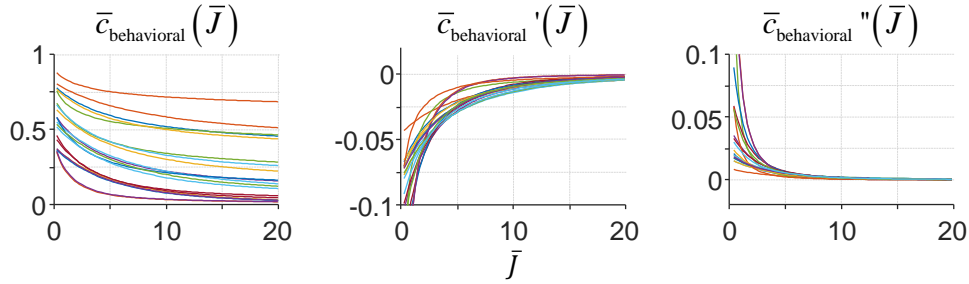
229
 230
 231

Supplementary Figures



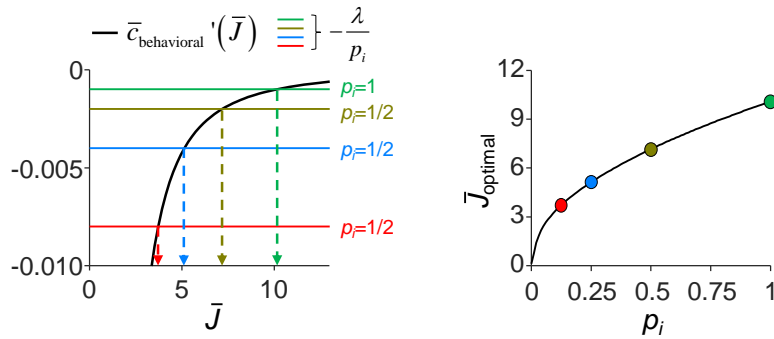
Supplementary figure S1. Fits to the three delayed-estimation benchmark data sets that were excluded from the main analyses. Circular variance (top) and circular kurtosis (bottom) of the estimation error distributions as a function of set size, split by experiment. Error bars and shaded areas represent 1 s.e.m. of the mean across subjects. The first three datasets were excluded from the main analyses on the ground that they were published in papers that were later retracted (Anderson & Awh, 2012; Anderson et al. 2011). The Rademaker et al. (2012) dataset was excluded from the main analyses because it contains only two set sizes, which makes it less suitable for a fine-grained study of the relationship between encoding precision and set size.

232



Supplementary figure S2. Examples of the expected behavioral cost function and its first and second derivative under a behavioral cost function $c_{\text{behavioral}}(\varepsilon)=|\varepsilon|^2$. Different colors represent different choices of parameters β and τ (randomly drawn).

233
234
235



Supplementary figure S3. Graphical illustration of the solution to the cost-minimization problem that determines the value of \bar{J}_{optimal} . The cost-minimizing value of solution of \bar{J} lies at the intersection between the derivative of the expected behavioral cost function (black curve) and a flat line at a value $-\lambda/p_i$ (colored lines). This value (indicated with arrows) necessarily increases with p_i . The parameter values used in this simulation were the same as in Fig. 1C of the main text.

236
237

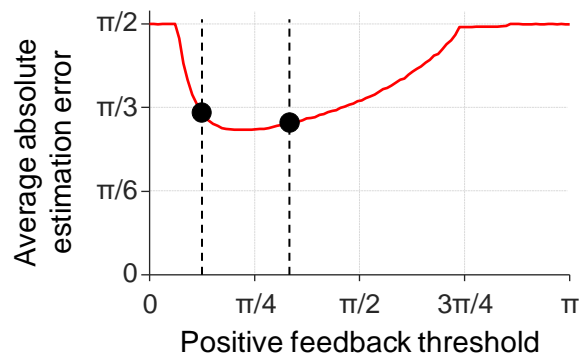


Figure S4. Model predictions for a delayed-estimation task with binary feedback ($N=5$). In this experiment, subjects receive positive feedback (e.g., “correct”) when their estimation error is smaller than the positive feedback threshold and negative feedback (e.g., “error”) otherwise. We modelled this using a behavioral cost function that maps errors below the feedback threshold to a cost of 0 and errors larger than this threshold to 1. The model predicts that subjects do not invest any resource when the threshold is very small or very large, such that the expected absolute estimation error is $\pi/2$ (guessing). This makes intuitive sense: for very small thresholds, the task is too difficult and for very large thresholds it is too easy to justify investing resource. In an intermediate regime, the prediction is U-shaped and contains a region in which the predicted estimation error barely changes as a function of feedback threshold. In this region, any performance benefit from increasing the amount of invested resource is almost exactly outdone by the added neural cost. The dashed lines show the feedback thresholds corresponding to the “high precision” and “low precision” conditions in the experiment by Nassar et al. (2017). Under the chosen parameter settings ($\lambda=0.008$, $\tau=30$), our model predicts that the average absolute estimation errors in these two conditions (black circles) are very similar to each other.

238
239
240

241 **Supplementary References**

242 Abramowitz, M., & Stegun, I. (1972). *Handbook of mathematical functions. Handbook of*
243 *Mathematical.*

244 Anderson, D. E., & Awh, E. (2012). The plateau in mnemonic resolution across large set sizes
245 indicates discrete resource limits in visual working memory. *Attention, Perception &*
246 *Psychophysics*, 74(5), 891–910. <https://doi.org/10.3758/s13414-012-0292-1>

247 Anderson, D. E., Vogel, E. K., & Awh, E. (2011). Precision in visual working memory reaches a
248 stable plateau when individual item limits are exceeded. *The Journal of Neuroscience*,
249 31(3), 1128–38. <https://doi.org/10.1523/JNEUROSCI.4125-10.2011>

250 De Silva, N., & Ma, W. J. (2018). Optimal allocation of attentional resource to multiple items
251 with unequal relevance. *BioRxiv*.

252 Keshvari, S., van den Berg, R., & Ma, W. J. (2013). No Evidence for an Item Limit in Change
253 Detection. *PLoS Computational Biology*, 9(2).

254 Mankiw, N. G. (2004). *Principles of economics. Book* (Vol. 328).
255 <https://doi.org/10.1017/CBO9780511511455>
256 Rademaker, R. L., Tredway, C. H., & Tong, F. (2012). Introspective judgments predict the
257 precision and likelihood of successful maintenance of visual working memory. *Journal of*
258 *Vision, 12*(13), 21. <https://doi.org/10.1167/12.13.21>
259